Journal of Control, Automation and Electrical Systems (2019) 30:113–124
https://doi.org/10.1007/s40313-018-00432-z

New Methodology for Evaluation of Non-pilot Relay Distance Protection

J. T. L. S Campos[1] · W. L. A Neves[2] · F. B. Costa[3] · D. Fernandes Jr.[2]

Received: 13 February 2018 / Revised: 11 December 2018 / Accepted: 12 December 2018 / Published online: 18 December 2018

Abstract
Distance relays are typically used in transmission line protection. Their accuracy depends on the correct relay parameterization, phasor estimators, and correct usage of distance characteristics. Identifying suitable relay parameterization and algorithms considering multiple transmission line with various topologies and different fault types is a hard task. Here, a methodology based on the relay trip performance is proposed to evaluate all the main concerns of distance protection such as: maloperation trips per relay units in each fault type, overreach operation, and maloperation due to faults closer to the relay. The methodology could identify the best phasor estimators and distance configurations among those evaluated, as well as it could verify the power system topologies which yield in challenges for distance protection. The results achieved by the proposed methodology demonstrated that it can be useful for assisting the development of phasor estimators and new distance characteristics, as well as for setting existing distance protection in specific power system topologies.

Keywords Distance protection · Relay algorithms · Phasor estimation

1 Introduction

Digital distance protection relay is based on the impedance estimation of the protected line, and it is the most widely used in transmission line protection because it is little affected by external events and it is easily coordinated (Power System Relaying Committee 2009). In addition, the distance protection does not need either a communication system to be connected to other relays or synchronization through GPS (Global Positioning System). One of the main concerns about the digital distance relays is the voltage and current phasor estimation, which ideally would be immune to the decaying Direct Current (DC) offset, harmonics, and inter-harmonics, as well as operate as fast as possible (Schweitzer et al. 2015). However, the well-known classical Fourier algorithm used for phasor estimation is not immune to the decaying DC offset (Schweitzer et al. 1993; Rosolowski et al. 2001; Campos et al. 2014). Therefore, with the increasing importance of digital relays, new phasor estimator algorithms appeared to overcome the classical Fourier problems. Modifications in the Fourier algorithm (Kang et al. 2009; ElRefaie and Megahed 2010) and the wavelet transform phasor estimators (Silva et al. 2010; Silva and Kusel 2012) were proposed.

The difficulty to choose an appropriate phasor estimator has been increasing due to the existence of too many algorithms, posing difficulties on the configuration of the most appropriate relay. In addition, specific power system topologies, such as double and multi-terminal lines, pose difficulties on relay settings. The mutual coupling in double lines causes ground relays to overreach in trip situations (Calero 2007).

Another concern is the correct choice of distance characteristic, which depends on the line load, expected fault resistance, and source impedance in both line ends (Sorrentino and De Andrade 2011). Therefore, the distance

✉ J. T. L. S Campos
joao.campos@unp.br

W. L. A Neves
waneves@dee.ufcg.edu.br

F. B. Costa
flaviocosta@ect.ufrn.br

D. Fernandes Jr.
damasio@dee.ufcg.edu.br

[1] Universidade Potiguar, Av. Nascimento de Castro, 1597 - Dix Sept Rosado, Natal, RN CEP 59054-180, Brazil

[2] Federal University of Campina Grande, R. Aprígio Veloso, 882 - Universitário, Campina Grande, PB CEP 58429-900, Brazil

[3] Campos Universitário, Lagoa Nova, Natal, RN CEP 59078-970, Brazil

characteristic design must address the aforementioned problems, which is done by several tests with different values of parameterization and usage of different types of characteristics.

Ideally, distance protection must operate only for faults within the predefined protection zone. However, in practice, the distance protection may not be accurate for all faults inside the protection zone because of reported issues such as high resistance faults, problems with phasor estimation (Pajuelo et al. 2010), problems with line compensation (Ghorbani 2015), and errors in the relay parameterization (Chen et al. 2017).

One solution to improve the relay performance is to improve the relay parameterization to be less sensitive to the aforementioned issues (Chen et al. 2017; Ma et al. 2017). However, the correct parameterization is not easy to pick and it depends on representative simulations, which may lead to protection coordination problems if a suitable parameterization is not obtained. Therefore, a methodology which gives a numerical value to the relay performance would be helpful to identify the most suitable parametrization.

There are papers which evaluate mho and quadrilateral relay dynamics under fault conditions (Kasztenny and Finney 2008; Alexander et al. 1991; Roberts et al. 1994), load flow influence in the distance relay performance (Alexander et al. 1991), phasor estimation affecting protection relays (Schweitzer et al. 2015), and distance protection in the presence of distributed generation (Campos et al. 2018). However, these works did not propose a methodology to evaluate distance protection considering several parameters at the same time such as distance characteristic functions, phasor estimation algorithms, and power system topologies.

This paper proposes a methodology based on indices to evaluate the relay performance considering representative fault simulations in different power system topologies. These indices focus on the desired distance relay performance in order to define which types of distance characteristics and phasor estimators are more suitable for a specific situation. Using the methodology, new phasor estimators as well as new distance characteristics can be tested and compared against each other to prove their efficiency.

Several faults were simulated using the IEEE power system proposed for protection testing (Power System Relaying Committee 2004). The mho and quadrilateral curves and various phasor estimators were evaluated by the proposed methodology considering various network topologies and fault types. According to the obtained results, the most appropriate relay configurations and phasor estimators depend on the power system topology. Also, the distance protection performance can be less affected by the fault conditions with the suitable relay configuration.

2 Digital Distance Protection Fundamentals

2.1 Phasor Estimation

Fourier-based algorithm is widely used by relay manufacturers for phasor estimation due to its harmonic filter capabilities (Schweitzer Engineering Laboratories 2007). However, it is affected by DC offset and inter-harmonics (Phadke and Thorp 2008). Therefore, changes in this algorithm or the usage of auxiliar algorithms are possible in order to overcome the DC offset problem, that is why Fourier-based algorithms are widely used by relay manufacturers. Examples of phasor estimators used by relays are one- and half-cycle Fourier algorithms with mimic filter, and the modified cosine algorithm (Hart et al. 2000).

The one-cycle Fourier (OCF) algorithm estimates a phasor as follows (Phadke and Thorp 2009):

$$Y_{\mathrm{re}}[k] = \frac{2}{N} \sum_{n=k-N+1}^{k} y[n] \cos(pn\theta), \tag{1}$$

$$Y_{\mathrm{im}}[k] = \frac{2}{N} \sum_{n=k-N+1}^{k} y[n] \sin(pn\theta), \tag{2}$$

where $Y_{\mathrm{re}}[k]$ and $Y_{\mathrm{im}}[k]$ are the real and imaginary parts of the phasor $\hat{Y}$ at sample k, i.e., $\hat{Y}[k] = Y_{\mathrm{re}}[k] + jY_{\mathrm{im}}[k]$; $N = f_{\mathrm{s}}/f$ is the number of samples per cycle, where f_{s} and f are the sampling and the fundamental frequency, respectively; $\theta = \frac{2\pi}{N}$ is the rotation angle; $y[n]$ is the sampled signal; and $p \in \mathbb{N}$, where $p = 1$ is the harmonic content for the fundamental estimation.

The half-cycle Fourier (HCF) algorithm uses half-cycle window to estimate the phasor as follows (Phadke and Thorp 2009):

$$Y_{\mathrm{re}}[k] = \frac{4}{N} \sum_{n=k-N/2+1}^{k} y[n] \cos(pn\theta), \tag{3}$$

$$Y_{\mathrm{im}}[k] = \frac{4}{N} \sum_{n=k-N/2+1}^{k} y[n] \sin(pn\theta). \tag{4}$$

The OCF and HCF do not filter the decaying DC component contained in fault currents properly. Therefore, the additional mimic filter can be included in the OCF and HCF algorithms (OCFM and HCFM) in order to overcome this problem as follows (Benmouyal 1995):

$$\hat{Y}^{*}[k] = K[(1+\tau_d)\hat{Y}[k] - \tau_d \hat{Y}[k-1]], \tag{5}$$

where $\hat{Y}^{*}[k]$ is the filtered phasor at sample k, $\hat{Y}[k]$ and $\hat{Y}[k-1]$ are the non-filtered phasors at samples k and $k-1$, respectively, τ_d is a time constant set by the user, and K is the filter gain.

In the power system, the mimic filter gain K is adjusted in order to set a unitary response for the fundamental frequency f as follows (Benmouyal 1995):

$$K = \sqrt{\frac{1}{(1+\tau_d-\tau_d\cos(\theta))^2+(\tau_d\sin(\theta))^2}}. \tag{6}$$

The modified cosine filter (MDC) is derived from the Fourier cosine filter (Hart et al. 2000), whose phasor ($\hat{Y}c = Yc_{\text{im}} + jYc_{\text{re}}$) is computed by:

$$\begin{aligned} &Yc_{\text{re}}[k] = Y_{\text{re}}[k] \\ &\quad and \quad Yc_{\text{im}}[k] = \frac{Y_{\text{re}}[k-1]-Y_{\text{re}}[k]\cos\theta}{\sin\theta}, \end{aligned} \tag{7}$$

where Yc_{re} and Yc_{im} are the MDC real and imaginary parts.

2.2 Distance Protection

The distance protection uses distinct unit groups with distance characteristics for different fault types: (1) phase-to-ground unit group (PG group), composed of AG, BG, and CG units, for single line-to-ground (SLG) faults (AG, BG, and CG faults); (2) phase-to-phase unit group (PP group), composed of AB, BC, and CA units, for line-to-line (LL), double line-to-ground (DLG), and three-line (LLL) faults (AB, BC, CA, ABG, BCG, CAG, and ABC faults). A specific relay unit (AG, BG, CG, AB, BC, or CA unit) can be activated through the combination of the overcurrent supervision and the fault selection logic according to the type of the fault.

The overcurrent supervision is usually based on phase and ground activators. The phase activator uses phase-to-phase currents ($\hat{I}_{AB}$, $\hat{I}_{BC}$, and $\hat{I}_{CA}$) to activate the units AB, BC, and CA, respectively, when a current threshold is reached. The ground activator uses the zero-sequence current ($\hat{I}_0$) in order to activate the relay ground units AG, BG, and CG. This supervision is important to avoid relay misoperations in high-load situations and to avoid relay phase units to be activated for single-ground faults (Schweitzer and Roberts 1993).

The fault selection logic selects the appropriate relay unit according to the fault. For instance, the fault selection can be given by Schweitzer and Roberts (1993):

$$angle(\hat{I}_0\hat{I}^{*}_{ph2}) < 50^{\circ}, \tag{8}$$

where $\hat{I}_{ph2}$ is the negative current in phase $ph = \{A, B \text{ or } C\}$. The relay identifies the phase when the above condition is satisfied. Fault selection is important to disable the relay ground units (AG, BG, and CG) DLG faults, and it is only applied to the relay ground units.

Due to the digital technology, the number of possible characteristic designs is very large. Historically, the relay manufacturers use the traditional distance characteristics (mho or quadrilateral) from the electromechanical relays since the relay setting knowledge is well known. Therefore, only mho- and quadrilateral-based distance protections are evaluated in this paper, whose torque equations for distance protection of the selected relay unit are given by (Kasztenny and Finney 2008):

$$\hat{S}_{R_{op}} = k_1\hat{I}_{R_{op}} + k_2\hat{V}_{R_{op}} \quad and \quad \hat{S}_{R_{pol}} = k_3\hat{I}_{R_{pol}} + k_4\hat{V}_{R_{pol}}, \tag{9}$$

where $\hat{S}_{R_{op}}$ and $\hat{S}_{R_{pol}}$ are the operation and polarization torque, respectively; k_1, k_2, k_3, and k_4 are parameters used to develop the distance characteristics; $\hat{I}_{R_{op}}$, $\hat{I}_{R_{pol}}$, $\hat{V}_{R_{op}}$, and $\hat{V}_{R_{pol}}$ are, respectively, the operation and polarization current and voltage phasors used by the relay, where $R = \{AG, BG, CG, AB, BC, CA\}$ representing each relay unit and their respective measured values. The relay will operate when:

$$\Re(\hat{S}_{R_{op}}\hat{S}^{*}_{R_{pol}}) > 0. \tag{10}$$

The directional element restricts the relay operation to faults in one direction and is usually used in both mho and quadrilateral functions. The reactance element restricts the reactance overreach by the mho characteristics and limits its reactance for quadrilateral functions. The right blinder restricts the resistance coverage by the quadrilateral function, whereas left blinder assures quadrilateral to not actuate for backwards faults.

The main distance characteristics such as directional, reactance, mho, right blinder, and left blinder can be designed through changes in $k_1, \ldots, k_4$, $\hat{I}_{R_{op}}$, $\hat{I}_{R_{pol}}$, $\hat{V}_{R_{op}}$, and $\hat{V}_{R_{pol}}$ in (9). For instance, Table 1 summarizes the values for the mostly used distance characteristics in the transmission lines protection (Ziegler 1999), where $\hat{Z}_{L1}$ is the positive sequence impedance from the protected line, which is used in the mho and reactance function parameters, $\hat{Z}_D$ is a directional setting used in the directional function parameters, $\hat{Z}_{BR}$ is a right blinder setting used in the right blinder function parameters, and $\hat{Z}_{BL}$ is a left blinder setting used in the left blinder function parameters.

The parameter m is usually set to 0.8% corresponding to 80% of the protected line impedance for the primary protection zone. The directional elements used in mho and quadrilateral functions use normally negative sequence currents $\hat{I}_{2R}$ for the current operation and the voltage polarization R measured by the relay. The reactance elements

Table 1 Parameter values for each distance characteristic

Characteristic	k_1	k_2	k_3	k_4	$\hat{I}_{R_{op}}$	$\hat{V}_{R_{op}}$	$\hat{I}_{R_{pol}}$	$\hat{V}_{R_{pol}}$
Mho	mZ_{L1}	-1	0	1	$\hat{I}_R$	$\hat{V}_R$	0	$\hat{V}_{mem_R}$
Mho reactance	mZ_{L1}	-1	Z_{L1}	0	$\hat{I}_R$	$\hat{V}_R$	$\hat{I}_{2R}$	0
Quad. reactance	mZ_{L1}	-1	Z_{L1}	0	$\hat{I}_R$	$\hat{V}_R$	$i\hat{I}_0 1^{j\theta}$	0
Directional	Z_D	0	0	1	$\hat{I}_{2R}$	0	0	$\hat{V}_R$
Phase selector	1	0	1	0	$\hat{I}_0$	0	$\hat{I}_{2R}$	0
Right blinder	Z_{BR}	-1	Z_{BR}	0	$\hat{I}_R$	$\hat{V}_R$	$\hat{I}_R$	0
Left blinder	Z_{BL}	-1	Z_{BL}	0	$\hat{I}_R$	$\hat{V}_R$	$\hat{I}_R$	0

are composed by the phase and ground reactance elements, in which the quadrilateral ground reactance element takes into account a homogeneity factor $1^{i\theta}$ in the zero-sequence current $\hat{I}_0$ (GE Energy 2012), whereas mho ground reactance element is only polarized using the negative sequence current. The phase and ground reactance elements use I_R operation currents for both mho and quadrilateral functions. The mho characteristic is usually polarized by a memory voltage $\hat{V}_{memR}$ in order to properly trip for LLL faults close in to the relay (Schweitzer 1992).

Additional logics can be implemented in the relay to overcome some typical problems (line capacitance compensation, protection through delta-wye transformers, misoperations in high-load condition) that distance relays can face. Examples of additional logics are loss of potential, switch on fault, load encroachment, delta-wye compensation, and capacitance compensation (Schweitzer Engineering Laboratories 2007).

In the relay ground units, the current phasor $\hat{I}_R$ in (9) must be compensated due to the mutual coupling between the transmission line faulted and unfaulted phases as follows (Ziegler 1999):

$$\hat{I}_{RC} = \hat{I}_R + \frac{\hat{Z}_0 - \hat{Z}_1}{\hat{Z}_1}\hat{I}_0, \tag{11}$$

where $\hat{I}_{RC}$ is the compensated current measured by the relay; $\hat{Z}_0$ and $\hat{Z}_1$ are the zero and positive sequence impedance of the protected line, respectively; $\hat{I}_0 = \hat{I}_A + \hat{I}_B + \hat{I}_C$ is the zero-sequence current of the protected line.

Parallel lines present additional mutual coupling. Therefore, the current $\hat{I}_R$ of the protected line must be compensated as follows [27]:

$$\hat{I}_{RC} = \hat{I}_R + \frac{\hat{Z}_0 - \hat{Z}_1}{\hat{Z}_1}\hat{I}_0 + \frac{\hat{Z}_{0m}}{\hat{Z}_1}\hat{I}_{02}, \tag{12}$$

where $\hat{Z}_{0m}$ is the zero mutual impedance between the lines; $\hat{I}_{02} = \hat{I}_{A2} + \hat{I}_{B2} + \hat{I}_{C2}$ is the zero-sequence current from the unprotected parallel line.

3 Proposed Methodology

The proposed methodology is based on two main evaluations: PP and PG relay units. Each phase relay has a dedicated evaluation and different behavior depending on the fault type, such as explained in the remainder of this section.

3.1 Relay Unit Status

The trip of the distance protection is generated by the relay unit groups according to the type of the fault as follows (Schweitzer and Roberts 1993):

- In SLG faults inside the protection zone, only the ground unit related to the faulted phase can trip (e.g., AG unit for AG faults).
- In DLG and LL faults inside the protection zone, only the phase unit related to the faulted phases can trip (e.g., AB unit for AB or ABG faults).
- In three-phase faults, only the phase units can trip, i.e., only AB, BC, and/or AC units must trip.
- The relay units cannot trip for faults outside the protection zone.

The proposed methodology takes into account the aforementioned interaction between the relay units (AG, BG, CG, AB, BC, and CA units) and all the faults (AG, BG, CG, AB, BC, CA, ABG, BCG, CAG, and ABC faults), and an index is associated with each relay unit in order to indicate whether the relay unit needs to actuate (status 1) or not (status 0) in a specific fault.

Table 2 summarizes the status of each relay unit and unit group for all fault types. For instance, the status of the relay unit AG is one for AG faults, resulting in the PG group with status 1, whereas the status of the other relay units is null. In ABC faults, for instance, the status of the relay units AB, BC, and CA is one, whereas the status of the relay units AG, B, and CG is null. With regard to the DLG faults, only the related phase-to-phase unit is one, i.e., no PG unit is activated since phase-to-ground unit overreaches for this fault type (Price

Table 2 Status of the relay unit groups

Fault type		Phase-to-ground				Phase-to-phase			
		Units			Group	Units			Group
		AG	BG	CG	PG	AB	BC	CA	PP
SLG	AG	1	0	0		0	0	0	
	BG	0	1	0	1	0	0	0	0
	CG	0	0	1		0	0	0	
LL	AB	0	0	0		1	0	0	
	BC	0	0	0	0	0	1	0	1
	CA	0	0	0		0	0	1	
DLG	ABG	0	0	0		1	0	0	
	BCG	0	0	0	0	0	1	0	1
	CAG	0	0	0		0	0	1	
LLL	ABC	0	0	0	0	1	1	1	1

and Einarsson 2008), whereas an ABG fault activates only the AB unit.

3.2 Indices for the Relay Performance Evaluation

The relay unit groups (PG and PP groups) are evaluated with overall performance, calculated through a weighted sum of indices depending on the relay status. Each index provides individual insight of the relay performance in the transmission line, i.e., it measures the importance of the relay performance in a specific situation based on the desired relay behavior, whereas the related weight quantifies the index importance.

The proposed indices Ind_{1G1}, Ind_{2GX}, Ind_{3GX}, and Ind_{4GX}, where $X = \{0, 1\}$ is the relay group status, are associated with the desired relay behavior, and they have special meaning, described as follows:

- Ind_{1G1} is associated with the efficiency of the trips (correct trips) provided by the relay group with status 1 for faults in the protection zone. Ideally, the relay must trip for all faults in the protected zone. An incorrect relay operation for faults inside the protection zone is supposed to be unacceptable for the protection system, resulting in underreach conditions. Therefore, Ind_{1G1} is one of the most important indices.
- Ind_{2GX} is associated with trips provided by relay units with status 0 belonged to relay group with status X for faults in the protection zone, which lead to a correct protection performance. Therefore, this wrong relay unit trip is only severe if single pole tripping is required. Otherwise, it is not severe because the relay tripped for the fault inside the protection zone.
- Ind_{3GX} is associated with trips provided by the relay for faults inside the transmission line, but outside the protection zone (wrong trip) by the relay group with status X. Such condition is not a major problem because the fault was inside the protected line, but it can lead to problems with protection coordination. Therefore, Ind_{3GX} is not considered to be severe. However, the proposed methodology penalizes the relay performance through Ind_{3GX} due to the overreached response of the distance protection.
- Ind_{4GX} is associated with trips provided by the relay for faults outside both the protection zone and protection line (wrong trips) by the relay group with status X. Ideally, the relay must not trip in these faults in order to avoid unnecessary out-of-service, which is unacceptable. Therefore, Ind_{4GX} is also one of the most important indices.

As a result of above indices description, the methodology computes the indices as follows:

$$Ind_{1G1} = C_T / N_{f1G1}, \tag{13}$$

$$Ind_{2GX} = Ind_{3GX} = Ind_{4GX} = 1 - (WT / N_{fyGX}), \tag{14}$$

where CT is the counted correct trips performed in N_{f1G1} fault simulations in the protection zone by the relay group with status 1, WT is the wrong trips performed in N_{fyGX} fault simulations by the relay group with status X in: (1) $y = 2$ (inside the protection zone); (2) $y = 3$ (inside the protected line but outside the protection zone); (3) $y = 4$ (outside the protected line).

3.3 Weights Associated with Indices

The indices have different importance since they evaluate different situations in the power system in order to represent each desired protection behavior. Each index is associated with a weight parameter (W_i) to determine its importance in the global relay performance.

Considering SLG, LL, and DLG Faults, the weights W_1, W_2, W_3, and W_4 are assigned to the indices Ind_{1G1}, Ind_{2G1}, Ind_{3G1}, and Ind_{4G1}, respectively, in the relay group with status 1, whereas in the relay group with status 0, the weights W_5, W_6, and W_7 are assigned to the indices Ind_{2G0}, Ind_{3G0}, and Ind_{4G0}, respectively. The weights in each group are normalized as follows:

$$\sum_{i=1}^{4} W_i = 1 \quad \text{and} \quad \sum_{i=5}^{7} W_i = 1. \tag{15}$$

For the LLL fault, the relay group evaluation does not have Ind_{2G1} index because all the PP relay units trip in this fault. Therefore, for this case, the weight W_8 is assigned to Ind_{1G1} instead of the W_1 and $W_8 = W_1 + W_2$.

As aforementioned, the weight value represents the index importance and this value needs to be assigned accordingly to their respective indices. Therefore, as Ind_{1GX} and Ind_{4GX} are the most important indices, their weight values need to be higher than the other indices. However, the weight value for each index is flexible and it will depend on the user needs for the relay parameterization.

3.4 Unit Group Evaluation

$$ES0_a = \sum_{i=5}^{7} W_{i;a} Ind_{i-3G0;a}, \tag{16}$$

$$ES0 = (ES0_X + ES0_Y + ES0_Z)/3, \tag{17}$$

where $ES0_a$ is a partial evaluation related to groups with status 0, in which $a = X, Y, Z$ are the phases of the unit group. For instance, in AG, BG and CG faults $X = AB$, $Y = BC$, and $Z = CA$, whereas for the other faults $X = AG$, $Y = BG$, and $Z = CG$; $ES0$ is the global evaluation for relay group with status 0, which is computed by the mean of partial evaluations $ES0_a$.

The relay group with status 1 global performance for SLG, LL, and DLG faults is given by:

$$ES1_{unit;Ind_{1G1}} = W_{1;unit} I_{1G1;unit}, \tag{18}$$

$$ES1_{b;Ind_{2G1}} = W_{2;b} Ind_{2G1;b}, \tag{19}$$

$$ES1_{c;Ind_{3G1},Ind_{4G1}} = \sum_{i=3}^{4} W_{i;c} I_{iG1;c}, \tag{20}$$

$$ES1 = ES1_{unit;Iind_{1G1}} + ES1_{b;Iind_{2G1}} + ES1_{c;Iind_{3G1},Iind_{4G1}}, \tag{21}$$

where $ES1_{unit,Ind_{1G1}}$ is the relay group evaluation with status 1 for Ind_{1G1}, where $unit$ represents the related relay unit with status 1. For instance, $unit = AG$ for AG faults, $unit = BG$ for BG faults, $unit = CG$ for CG faults, $unit = AB$ for AB and ABG faults, $unit = BC$ for BC and BCG faults, $unit = CA$ for CA and CAG faults; $ES1_{b;Ind_{2G1}}$ is the relay group evaluation with status 1 for Ind_{2G1}, and it is computed by the mean of the relay partial evaluations contained in b, in which b is the relay units Y and Z belonging to the group with status 0, but with unit status 0. For instance, in AG faults $Y = BG$ and $Z = CG$, whereas in AB faults $Y = BC$ and $Z = CA$; $ES1_{c;Ind_{3G1},Ind_{4G1}}$ is a partial evaluation with status 1 for Ind_{3G1} and Ind_{4G1}, in which $c = X, Y, Z$ is the phases of the unit group. Regarding three-phase faults, just the global performance of the relay group with status 1 is evaluated by:

$$ES1_{LLL} = ES1_{X;Ind_{1G1}} + ES1_{c;Ind_{3G1},Ind_{4G1}}, \tag{22}$$

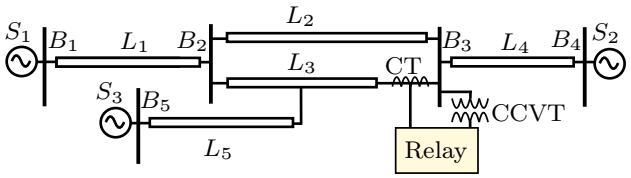

Fig. 1 Adopted power system (Power System Relaying Committee 2009)

where $ES1_{LLL}$ is the relay group evaluation with status 1 for LLL faults. In these faults, the Ind_{2G1} is not taken into account due to all relay units of the group operate at the same time.

4 Modeling and Simulations

4.1 The Power System Modeling

The relay performance was evaluated in the power system proposed by the IEEE (Power System Relaying Committee 2004) (Fig. 1) through time-domain simulations in an electromagnetic transient program (EMTP). The transmission lines L_1, L_2, L_3, L_4, and L_5 were modeled with frequency dependent distributed parameters and assuming ideal transposition. The sources S_1, S_2, and S_3 were modeled with lumped parameters calculated at the frequency of 60 Hz. The length of lines L_2 and L_3 is 300 km, whereas the length of L_1, L_4, and L_5 is 100 km. Moreover, L_5 is connected at the middle of line L_3. The power system has five buses, namely B_1, B_2, B_3, B_4, and B_5. More details about the power system model such as the line parameters can be found in Power System Relaying Committee (2004).

The relay performance was evaluated with power system load conditions summarized in Table 3 and with different topologies of the power system:

- topology 1: L_2 and L_5 disconnected (single line);
- topology 2: L_5 disconnected (double line);
- topology 3: all lines connected (tapped line).

4.2 The Relay Parameters

The analog filter of the modeled relay was a second-order analog Butterworth filter with a cutoff frequency of 480 Hz for a 960 Hz sampling frequency. On the other hand, the A/D conversion was assumed to be ideal, resulting a non-additional error source. The used phasor estimators were the MDC, HCF, HCFM, and OCFM, in which the mimic filter time constant was set to one for the fundamental cycle ($\tau_d = 16$).

Table 3 Source parameters

Source	S_1	S_2	S_3
Voltage (pu) base 230 kV	$1.05\angle 10°$	$1.05\angle -10°$	$1.05\angle 10°$
$Z(\Omega)$	$0.35 + j3.15$	$0.35 + j4.12$	$0.35 + j4.12$

Table 4 Characteristics settings

Topology	Mho			Quadrilateral			
	Mho	Reactance	Directional	Right blinder	Left blinder	Reactance	Directional
1, 2	$0.8L_3$	$0.8L_3$	$1\angle L_3$	$100\angle 0°$	$10\angle 180°$	$0.8L_3$	$1\angle L_3$
3	$0.4L_3$	$0.4L_3$	$1\angle L_3$	$100\angle 0°$	$10\angle 180°$	$0.4L_3$	$1\angle L_3$

The distance protection was activated by phase- and ground-overcurrent activators (GE Energy 2012): the threshold for the phase-to-phase currents was 600 A (10% higher than the load current), whereas the threshold of the ground current was of 100 A, which is higher than the noise presented in the relay signals to prevent the relay to be activated in the presence on non-ground fault situation (GE Energy 2012).

The relay was located at bus B_3 in order to protect the line L_3. The adopted mho- and quadrilateral-based distance function parameterizations are summarized in Table 4. The mho and the reactance characteristics were set to protect the line L_3 at 80% of the line length for the topologies 1 and 2. For the topology 3, the mho and reactance characteristics were set to protect 40% of the L_3 length. The directional angle for the directional characteristic was set to be equal to the angle of the impedance of the line L_3. According to Schweitzer Engineering Laboratories (2011), the right blinder setting does not have a defined value, and the relay parametrization will depend of the desired coverage resistance, which depends on statistic studies and expertise. In this paper, the right blinder was set to 100 Ω in order to be conservative and trip for faults with resistance up to 100 Ω (Calero et al. 2010). The left blinder relay was set to 10 Ω for a good back coverage. The impedance angle of the directional relay is equal to the line L_3 to be protected. The reactance relay was set to 80% of the L_3 length. The mho and quadrilateral protections are polarized by the IIR filter presented in Schweitzer (1992).

4.3 Fault Simulation

Faults were simulated in different locations of the power system in order to evaluate the proposed methodology (Table 5). The faults were simulated on lines L_1, L_2, L_3, L_4, and L_5, as well as on buses B_2 and B_3 depending on the adopted topology. Since the faults were simulated near the buses, near 80% of the protection zone for topologies 1 and 2, and near 40% of the protection zone for topology 3, the relay was evaluated in the worst fault scenarios for the distance protection. Since the used power system is balanced, there was no need to apply all fault types, i.e., the simulated fault types were AG, AB, ABG, and ABC.

A total of 1368 faults were simulated in the topology 1 (single line configuration), considering the locations 15, 25, 50, 200, 210, 220, 230, 240, 250, 260, and 270 km on line L_3 and 15, 25, 50, and 75 km on lines L_1 and L_4. In each fault location, the ground and phase resistances were 0, 1, 5, 10, 50, 100 Ω with fault inception angle of 0, 45, and 90 degrees for the fault types AG, AB, ABG, and ABC. The same fault configuration was simulated in buses B_2 and B_3. A total of 2160 faults were simulated in the topology 2 (double line configuration), in which the line L_2 is in parallel to line L_3. The fault configuration in this topology was the same for topology 1, but with additional faults simulated in L_2. The line L_5 was added at the middle (150 km) of the line L_2 in the topology 3 (tapped line configuration). The faults on lines L_2 and L_3 were simulated in 15, 25, 50, 100, 110, 120, 125, 130, 145, 155, 170, and 230 km from the bus 2. The faults on the line L_5 were located 15, 25, 50, and 75 km from the intersection point. A total of 2592 faults were simulated in the topology 3.

5 Performance Assessment

The proposed methodology used the default weights presented in Table 6. The chosen weights were based on a statistical study where they were submitted to high disturbances in order of 50% in each weight and the methodology, shown to be not biased, presented a maximum error deviation of 6.21% in the final results.

The trips collected in the simulations were analyzed by the proposed methodology, and a global performance was computed for identifying the best distance protection settings and phasor estimators in topologies 1, 2, and 3.

Tables 7, 8, and 9 summarize the relay phase-to-ground and phase-to-phase global performance provided by the proposed methodology for each relay configuration in the used

Table 5 Simulated faults

Topologies	Description	
1, 2, and 3	Fault type	AG, AB, ABG, and ABC
1, 2, and 3	Θ_f (degrees)	0, 45, 90
1, 2, and 3	R_g and R_p (Ω),	0, 1, 5, 10, 50, 100
1, 2, and 3	Fault location (km)	15, 25,
	(L_1, L_4, L_5)	50, 75
1 and 2	Fault location (km)	15, 25, 50, 200, 210, 220,
	(L_2, L_3)	230, 240, 250, 260, 270
3	Fault location (km)	15, 25, 50, 100, 110, 120,
	(L_2, L_3)	125, 130, 145, 155, 170, 230

Table 6 Default weights

W_1 (%)	W_2 (%)	W_3 (%)	W_4 (%)	W_5 (%)	W_6 (%)	W_7 (%)	W_8 (%)
40	5	10	45	10	20	70	45

Table 7 Relay phase-to-phase comparison between HCF and HCFM using quadrilateral curve

Top.	SLG fault	LL fault		DLG fault		LLL fault	
	HCF/HCFM (%)	HCF (%)	HCFM (%)	HCF (%)	HCFM (%)	HCF (%)	HCFM (%)
1	100	74.29	89.74	74.17	89.82	71.07	88.27
2		88.55	88.63	74.05	88.97	71.07	85.83
3		88.26	90.11	88.38	89.72	87.33	87.83

power systems topologies, which is useful for verification of the best characteristic, phasor estimator, etc.

The performance of the quadrilateral-based distance protection was evaluated through the proposed methodology by considering the half-cycle Fourier algorithm with and without mimic filter as summarized in Table 7. The HCF presented the worst performance (18% lower than the HCFM) as expected. Therefore, the proposed methodology based on indices could identify unappropriated phasor estimators (HCF is affected by DC offset components when no additional filtering is used Phadke and Thorp 2008) for distance protection.

Regarding the usual phasor estimators, the MDC and OCFM phasor estimators presented results close to each other, whereas the HCFM presented the best performance. However, HCFM presented some wrong trips (few internal DLG faults were not detected) in the phase-to-ground relay unit evaluation. Therefore, the selection of the best phasor estimator, which is one of the key points in the distance protection, can be properly assisted by the proposed methodology.

According to Tables 8 and 9, both quadrilateral and mho characteristics presented 100% of success rate for faults outside the protected line (no external fault detected). Regarding the faults inside the protected line, quadrilateral function presented superior performance than the mho function independent of the phasor estimator and the type of fault due to its higher resistance coverage. Therefore, the proposed methodology can be properly used for identification of the best characteristic of the distance protection.

Although the quadrilateral characteristic was better than the mho, there are situations where mho can be better than the quadrilateral. For instance, based on Roberts et al. (1994) the mho- and quadrilateral-based distance relays were evaluated by the methodology in high-load conditions in topology 1, which corresponds to $S_1 = 1.05\underline{/30°}$ and $S_2 = 0.95\underline{/-30°}$ ($\Delta\delta = 60°$). Table 10 summarizes the relay performance using the methodology in high-load conditions. Quadrilateral characteristic presented better performance for SLG faults, whereas mho presented better results for LL, DLG, and LLL faults for relay group with status 1. The mho and quadrilateral characteristics reached 100% of success rate for relay group with status 0. The methodology indicated that the quadrilateral characteristic was the most affected by high-load conditions when relay phase-to-ground units are disabled.

The proposed methodology indicates improvements in the used phasor estimators and distance characteristics. Such improvements are possible through the change of relay settings or additional functions such as the load encroachment (Roberts et al. 1994), but the search for the ideal distance protection is out of scope of this paper.

Table 8 Relay phase-to-ground results with proposed methodology

Topology	MDC		HCFM		OCFM		MDC		HCFM		OCFM	
	MHO (%)	QUAD (%)	MHO (%)	QUAD (%)	MHO (%)	QUAD (%)	MHO (%)	QUAD (%)	MHO (%)	QUAD (%)	MHO (%)	QUAD (%)
	SLG fault						LL fault					
1	85.62	87.44	86.57	87.96	83.85	88.00	100					
2	85.79	87.44	86.88	88.53	85.75	87.72						
3	83.65	87.92	83.65	88.43	83.79	88.43						
	DLG fault						LLL fault					
1	100		99.93	99.97	100							
2			99.83	99.89								
3			99.98	99.99								

Table 9 Relay phase-to-phase results with proposed methodology

Topology	MDC		HCFM		OCFM		MDC		HCFM		OCFM	
	MHO (%)	QUAD (%)	MHO (%)	QUAD (%)	MHO (%)	QUAD (%)	MHO (%)	QUAD (%)	MHO (%)	QUAD (%)	MHO (%)	QUAD (%)
	SLG fault						LL fault					
1	100						86.45	88.97	87.96	89.74	86.79	89.25
2							86.05	88.55	87.06	88.63	86.23	88.69
3							83.58	88.26	84.92	90.11	83.72	89.43
	DLG fault						LLL fault					
1	86.45	88.85	87.70	89.82	86.45	89.11	85.24	86.83	85.25	88.27	86.31	87.24
2	86.45	88.31	86.69	88.97	86.31	88.45	84.64	84.35	84.50	85.83	84.50	84.88
3	84.92	88.38	84.92	89.72	83.72	89.10	82.32	87.33	83.75	87.83	82.46	88.25

Table 10 Relay comparison between Mho and quadrilateral with high-load conditions ($\Delta\delta = 60°$) in topology 1

Fault Type	Phase-to-ground units		Phase-to-phase units	
	MHO (%)	QUAD (%)	MHO (%)	QUAD (%)
SLG	71.43	77.50	100	
LL	100		72.92	69.75
DLG	100		72.83	69.75
LLL	100		69.33	65.00

With regard to the topology influence in the relay performance, the worst distance protection performance was in topology 3 (tapped line), whereas topologies 1 (single line) and 2 (double line) presented similar performance. The methodology provided an insight into the influence of the power system in the relay performance, which is helpful for defining strategies to overcome this possible issue. One solution to improve relay performance for tapped lines can be the increasing of the relay range Alexander and Andrichak 1996. In order to ensure whether the range increase is a good strategy, the methodology can be computed and a comparison with previous value can be done.

The group evaluation with status 0 (the relay phase-to-ground units for LL, DLG, and LLL faults in Table 8 and the relay phase-to-phase units for SLG in Table 9) presented good performance, where almost 100% success rate was obtained for all fault types.

The relay group evaluation with status 1 (relay phase-to-ground units for SLG faults in Table 8 and relay phase-to-phase units for LL, DLG, and LLL faults in Table 9) did not present 100% in any case, but the results were higher than 80% in almost all the cases. However, these results were expected due to the simulation of high resistance faults (higher than 50 Ω), which leads the distance protection to operate in its limit (Calero et al. 2010). The increase in the relay resistance coverage is one possible solution to obtain results closer to 100% (Calero et al. 2010). However, this solution can lead to relay misoperations in high-load situations (IEEE 2016).

6 Case Studies

The proposed methodology has a potential to support both distance relay settings and pilot protection after some improvements. For instance, two case studies are shown in this section in order to verify new application possibilities of the proposed methodology. In these case studies, faults presented in Table 11 were simulated in the power system 1 with the topology 1 (lines L_2 and L_5 are disconnected), and the methodology was evaluated considering the phasor estimator with modified cosine and the MHO characteristic.

Table 11 Simulated faults in case studies 1 and 2

Description	
Fault type	AG
Θ_f (degrees)	0, 45, 90
R_g and R_p (Ω),	0, 1, 5, 10, 50, 100
Fault location (km)	15, 25,
(L_1, L_4, L_5)	50, 75
Fault location (km)	15, 25, 50, 200, 210, 220,
(L_2, L_3)	230, 240, 250, 260, 270

Table 12 Relay performance for settings on 40% and 80% of the line length

Indices	Relay settings	
	40%	80%
$ES1_{a;Ind1G1}$	14%	32%
$ES1_{b,c;Ind2G1}$	5%	5%
$ES1_{Ind3G1}$	10%	8%
$ES1_{Ind4G}$	45%	45%
Total performance	74%	91%

6.1 Case Study 1: Possibility to Support Relay Settings

In this case study, the relay is located in the bus 3 in order to protect the line L_3. It is well known that the distance protection usually is set to protect 80% of the line length in this type of power system topology. However, the relay protection was intentionally set to protect only 40% of the line length, i.e., a wrong setting, with the aim to show that the proposed methodology can be used to identify wrong relay protection settings. The relay with correct settings on 80% of the line length was also considered for comparison.

Table 12 presents the obtained results for each proposed index considering these two settings (40% and 80%), where the total performance is given by the sum of the indices.

According to Table 12, the relay setting with 40% presented the worst results. Assuming that the phasor estimator and distance characteristics are well fitted, the results indicate that there are errors in the relay settings. In this case, the relay set to 40% does not trip for all the faults inside in 80% of the protection zone 1. These results show that the proposed methodology could be used by the power system utilities to both validate relay settings and alert when settings are not suitable. Therefore, the proposed methodology can be improved to be used in these types of applications in future works.

Table 13 Case study 2: POTT-based protection results

Relay units	Results
$ES1_{a;Ind1G1}$	46%
$ES1_{Ind4G}$	40%
Total performance	86%

6.2 Case Study 2: Possibility to be used in the Pilot Protection

In extra-high voltage transmission lines, the principal protections are pilot-based protections such as: permissive overreaching transfer trip (POTT) or directional comparison blocking (DCB) because fast fault clearance is needed to protect the entire line Schweitzer and Kumm 1996.

As a case study, a modification in the proposed methodology was accomplished to evaluate a distance function in association with the POTT protection: the proposed indices $ES1_{Ind2G1}$ and $ES1_{Ind3G1}$ are not taken in account because in this protection scheme the remote and local relays are set to 120 % of the protected line length in order to protect the entire line (reach of 100%) in an AND combination of individual protections. The index $ES1_{a;Ind1G1}$ was set to a weight of 0.6 and for the index $ES1_{Ind4G}$ a weight of 0.4 was used. These weights can be different depending of the main purpose of the power system operator. In this case study, the index $ES1_{a;Ind1G1}$ evaluates all trips inside the protection zone, which was considered to be 100 % of the protected line length. The index $ES1_{Ind4G}$ evaluates all wrong trips outside the protection zone.

Table 13 presents the results obtained with the modified methodology. In this case study, the local relay is located in the bus 3 and the remote relay is located in the bus 2, both protecting the line L_3.

According to the results presented in Table 13, the modified methodology alerts that POTT was not actuate for all faults inside the protected line which is consistent with the simulated faults with high resistance. Despite the 100 % line length reach, the POTT protection could not detect high resistance faults in the protected line. A possible solution can be the increasing of the POTT settings. However, the main purpose of this case study is only to guide a possible usage of the methodology in new scenarios in pilot protection, which is outside of the scope of the paper.

Based on this case study, as future works, the proposed methodology can be adapted to include pilot protection schemes by using new indices. In POTT and DCB protections, for instance, three indices can be defined: an index to measure relay trips in faults inside the protected line, an index to measure relay trips in faults outside the protected line, and an index to measure relay operating time in faults inside the protected line. Additionally, the chosen weights have to be representative according to the importance of each index.

7 Conclusion

A novel methodology for evaluation of digital distance relay algorithms based on correct and wrong trips was proposed. Fault simulations were performed in a system proposed by IEEE varying the fault inception angle, distance, type, and resistance in three power system configurations: single line, double line, and tapped line. In the relay architecture, three phasor estimators were used for showing the influence of digital filters, and two distance protection configurations were considered for evaluating the resistance coverage. The methodology could identify the best distance protection characteristic, the best phasor estimator for a specific power transmission line, and the power system topologies in which the distance relays may face more problems. Regarding the distance relay characteristic, the proposed methodology suggested that the quadrilateral was usually better than the mho. However, there are situations where mho can be better. Regarding the phasor estimation, the proposed methodology identified that the Fourier-based method without mimic filter presented inferior performance due to the influence of the DC offset, whereas the results of the half- and one-cycle Fourier with mimic filter and the modified cosine were compatible, suggesting that the characteristics have a main contribution to the relay global performance when the phasor estimator is selected accordingly.

According to the proposed methodology, the tapped line provided more challenges for the distance protection, whereas single and double lines presented similar performance in the evaluated scenario, although the relay can be affected by the mutual coupling effect of double lines. The adopted relay configuration influenced in the results suggesting that different algorithms and characteristics can be adopted depending on the fault type. Also, high-load conditions affected distance characteristics being the quadrilateral the most affected.

Since the proposed methodology could identify the best distance protection characteristic and phasor estimator as well as the power system topologies in which the distance relays may face more problems, this methodology can be used to verify the best commercial distance relays in future works.

Acknowledgements The authors would like to thank CAPES and CNPq for the financial support.

References

Alexander, G. E., & Andrichak, J. G. (1996). Application of phase and ground distance relays to three terminal relays. Technical report, GE Protection & Control Malvern.

Alexander, G. E., Andrichak, J. G., Malvern, P. A., & Annual, N. (1991). Ground distance relaying: Problems and principles. In *Eighteenth annual western protective relaying conference*, October.

Benmouyal, G. (1995). Removal of DC-offset in current waveforms using digital mimic filtering. *IEEE Transactions on Power Delivery*, *10*(2), 621–630.

Calero, F. (2007). Mutual impedance in parallel lines—Protective relaying and fault location considerations. In *34th annual western protective relay conference*.

Calero, F., Guzman, A., & Benmouyal, G. (2010). Adaptive phase and ground quadrilateral distance elements. Technical report, Schweitzer Engineering Laboratories.

Campos, J., et al. (2018). Distance protection analysis applied for distribution system with distributed generation. *Przeglad Elektrotechniczny* 94

Campos, J. T. L. S., Neves, W. L. A., Fernandes, D., & Costa, F. B. (2014). Methodology for evaluation of relay digital filters during a fault. In *2014 IEEE PES general meeting—Conference exposition* (pp. 1–5).

Chen, S., Tai, N., Fan, C., Liu, J., & Hong, S. (2017). Adaptive distance protection for grounded fault of lines connected with doubly-fed induction generators. *IET Generation, Transmission & Distribution*, *11*(6), 1513–1520. 4 20.

ElRefaie, H. B., & Megahed, A. I. (2010). A novel technique to eliminate the effect of decaying DC component on DFT based phasor estimation. In *2010 IEEE power and energy society general meeting*.

GE Energy. (2012). D30 line distance protection system instruction manual.

Ghorbani, A. (2015). An adaptive distance protection scheme in the presence of phase shifting transformer. *Electric Power Systems Research*, *129*, 170–177.

Hart, D. G., Novosel, D., & Smith, R. A. (2000). Modified cosine filters

IEEE. (2016). IEEE guide for protective relay applications to transmission lines, IEEE Std C37.113-2015 (Revision of IEEE Std C37.113-1999) (pp. 1–141).

Kang, S.-H., Lee, D.-G., Nam, S.-R., Crossley, P. A., & Kang, Y.-C. (2009). Fourier transform-based modified phasor estimation method immune to the effect of the DC offsets. *IEEE Transactions on Power Delivery*, *24*(3), 1104–1111.

Kasztenny, B., & Finney, D. (2008). Fundamentals of distance protection. In *2008 61st annual conference for protective relay engineers*.

Ma, J., Xiang, X., Li, P., Deng, Z., & Thorp, J. S. (2017). Adaptive distance protection scheme with quadrilateral characteristic for extremely high-voltage/ultra-high-voltage transmission line. *IET Generation, Transmission & Distribution*, *11*(7), 1624–1633. 5 11.

Pajuelo, E., Ramakrishna, G., & Sachdev, M. S. (2010). Strengths and limitations of a new phasor estimation technique to reduce CCVT impact in distance protection. *Electric Power Systems Research*, *80*(4), 417–425.

Phadke, A., & Thorp, J. (2008). *Synchronized phasor measurements and their applications, power electronics and power systems*. Berlin: Springer.

Phadke, A. G., & Thorp, J. S. (2009). *Computer relaying for power systems* (2nd ed.). Hoboken: Wiley.

Power System Relaying Committee. (2004). EMTP reference models for transmission line relay testing report, draft 10a, Technical report.

Power System Relaying Committee. (2009). Understanding microprocessor-based technology applied to relaying. Technical report.

Price, E., & Einarsson, T. (2008). The performance of faulted phase selectors used in transmission line distance applications. In *2008 61st annual conference for protective relay engineers* (pp. 484–490).

Roberts, A., Guzman, J., & Schweitzer, III, E. O. (1994). Z = v/i does not make a distance relay. In *48th annual Georgia tech protective relaying conference*.

Rosolowski, E., Izykowski, J., & Kasztenny, B. (2001). Adaptive measuring algorithm suppressing a decaying DC component for digital protective relays. *Electr. Power Syst. Res.*, *60*(2), 99–105. 16.

Schweitzer Engineering Laboratories. (2007). SEL-311C relay, protection and automation system instruction manual.

Schweitzer Engineering Laboratories. (2011). SEL-421 relay protection and automation system—Instruction manual.

Schweitzer III, E. O. (1992). Distance relay using a polarizing voltage.

Schweitzer III, E. O., & Hou, D. (1993). Filtering for protective relays. In *IEEE WESCANEX 93 communications, computers and power in the modern environment*.

Schweitzer III, E. O., & Kumm, J. J. (1996). Statistical comparison and evaluation of pilot protection schemes. In: *Proceedings of the 23rd annual western protective re-lay conference*, Spokane, WA.

Schweitzer III, E. O., Kasztenny, B., Guzman, A., Skendzic, V., & Mynam, M. V. (2015). Speed of line protection can we break free of phasor limitations? In *Annual conference for protective relay engineers*.

Schweitzer, E. O, I. I. I., & Roberts, J. (1993). *Distance relay element design*. Texas.

Silva, K. M., & Kusel, B. F. (2012). On combining wavelet-based designed filters and an adaptive mimic filter for phasor estimation in digital relaying. *Electric Power Systems Research*, *92*, 60–72.

Silva, K. M., Neves, W. L. A., & Souza, B. A. (2010). Distance protection using a wavelet-based filtering algorithm. *Electric Power Systems Research*, *80*(1), 84–90.

Sorrentino, E., & De Andrade, V. (2011). Optimal-probabilistic method to compute the reach settings of distance relays. *IEEE Transactions on Power Delivery*, *26*(3), 1522–1529.

Ziegler, G. (1999). *Numerical distance protection: Principles and application*. Munich: Publicis MCD.